

Proceedings

Part 2

INTERNATIONAL
AEGEAN CONFERENCE
ON

ELECTRICAL MACHINES and POWER ELECTRONICS

Kuşadası, TÜRKİYE

27 - 29 May 1992

Organized by: Middle East Technical University
Ankara, Türkiye

Sponsored by: Turkish Scientific and Technical Research Council
ABB Asea Brown Boveri Türkiye
TEE Turkish Electrical Industry Co.
Barmek Holding

General Expressions for Forces Acting in EDS-MAGLEV Systems Driven
by Linear Synchronous Motors

M.Andriollo, G.Martinelli, A.Morini
Department of Electrical Engineering, University of Padova
Via Gradenigo 6/a - I-35131 Padova - ITALY

Abstract

In the paper the levitation, drag and lateral forces acting on EDS-MAGLEV vehicles are determined using an analytical three-dimensional method which takes into account all the types of coil configurations already realized and under development.

1 Introduction

High-speed magnetically levitated ground transportation (MAGLEV) can be utilized for intercity travels of the order of some hundreds km (as an alternative to high-speed on-rail trains, motor cars and short-haul commercial flights) as well as for speedy connections between airports or shuttle services between airports and downtown [1].

In EDS-MAGLEV systems the levitation of the vehicle derives from the repulsive force due to the interaction between on-board superconducting (SC) magnets and currents induced in short-circuited ground coils. The vehicle is propelled by air-cored long-stator linear synchronous motors (LSM) with SC field windings; the speed adjustment is attained by a variable frequency stator supply, using static converters [2].

The results of the experimental activity on prototypes achieved in Japan [3] have proved that the basic MAGLEV technology has almost attained a level of immediate practical use. In Yamanashi Prefecture is under design and construction the first commercial 44 km-long test line, as a part of the 500 km-Linear Express, which, at the beginning of next century, should connect Tokyo and Osaka by means of MAGLEV trains, having 14+16 cars and running at 500 km/h [4].

In the paper the levitation, drag and lateral forces acting on EDS-MAGLEV vehicles are determined, using an analytical three-dimensional method which allows to consider all types of coil configurations used in the systems. The resulting analytical expressions, developed for the actual case of coils with finite thicknesses as well as for the approximated case of filiform coils, are, unlike [5], the most general and take into account the various coil configurations simply by changing suitable coefficients. The approximation of filiform coils allows to develop simpler expressions with a usually satisfactory precision. The utilization of analytically-developed general expressions allows to perform, unlike numerical methods, a quick and easy evaluation of the forces when the coil sizes and configurations vary (parametric analyses).

As an example, the paper finally gives the levitation, drag and lateral forces obtained applying the developed expressions to some configurations.

2 Types of configurations

In an EDS-MAGLEV transport system, many main winding systems are present, which may be represented by series of rectangular-shaped coils [5,6]:

- 1 - Series of on-board SC field coils: they produce the excitation field of the LSM.
- 1a - Series of on-board levitation SC coils: they produce the field necessary for the levitation unless the excitation field itself is used for such purpose.
- 2 - Series of on-ground armature coils: they produce the propulsion force interacting with coils 1).
- 3 - Series of on-ground levitation coils: they produce the levitation force interacting with coils 1) or 1a).

Field 1 and armature 2 coils systems of the LSM

Fig.1 shows the SC field and the armature windings of the LSM, with reference to one side of the vehicle. The field and armature coils are on parallel vertical planes: the former are grouped in opposite polarity pairs and the latter, equally spaced, in three phases.

Field 1 and on-ground levitation 3 coils systems on orthogonal planes

Fig.2 shows the on-board SC field winding and the on-ground levitation coils, with reference to one side of the vehicle. The levitation coils, equally spaced and short-circuited, are on a horizontal plane, orthogonal to the vertical one of the field coils.

Given a reference system fixed to the vehicle, X,Y,Z are the coordinates of a generic levitation coil with respect to 0; supposing the speed v constant, it results that:

$$Y = Y_0 - vt$$

where Y_0 is the value of Y at $t=0$.

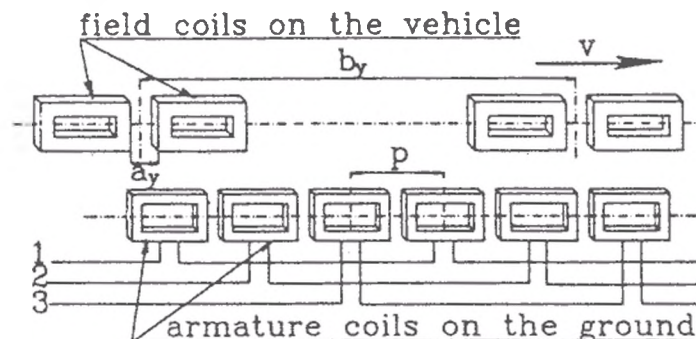


Fig.1 - Field and armature coils of the LSM [a : distance between the two field coils of a pair; b_y : polar pitch; $p=b_y/3k$: armature coils pitch; (k: number of armature coils per phase and polar pitch); 1,2,3: armature phases].

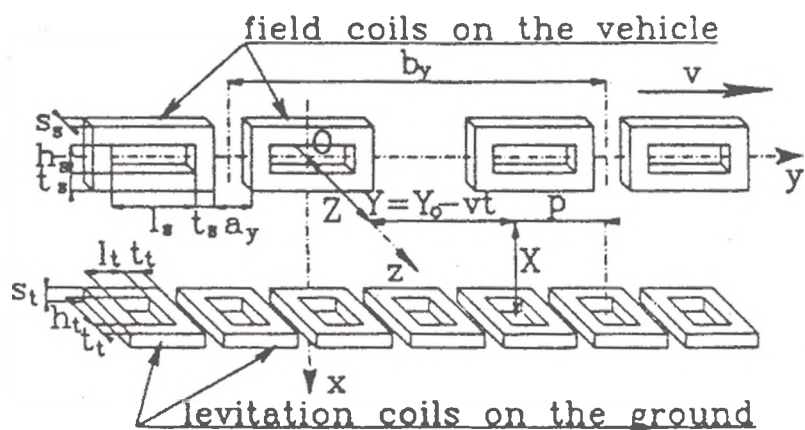


Fig. 2 - Field and levitation coils on orthogonal planes [l_s, h_s, s_s, t_s : field coils dimensions; a_y : distance between the field coils of a pair; b_y : polar pitch; l_t, h_t, s_t, t_t : levitation coils dimensions; $p = b_y/N$: levitation coils pitch (N : number of coils per polar pitch and side)].

On-board SC 1a and on-ground levitation 3 coils systems on parallel and horizontal planes

Fig. 3 shows another proposed configuration, in which a second series of SC coils is on-board, in addition to the SC field winding; such coils are horizontal and parallel to the on-ground levitation coils.

Field 1 and on-ground levitation 3 coils systems on parallel and vertical planes

Fig. 4 shows another proposed configuration, in which the on-ground levitation coil is composed of two unit coils, arranged in two rows up and down and connected in reverse direction to form an 8-shaped coil. When the center of a SC coil matches that of the 8-shaped coil (vertical displacement $X=0$), the magnetic flux through it is null. In addition the 8-shaped coils on both sides of the guideway are connected reversely to make a null-flux circuit: the current flowing in it, when a lateral displacement occurs, improves the stability. In case the vehicle is centered with respect to the guideway ($\Delta Z=0$), the current is null and the distance between the levitation and the field coils is Z_0 both for the left and the right sides.

3 Forces between coils on orthogonal planes

With reference to Fig. 2, the coefficient of mutual inductance M_{ts} between the field coils and a generic levitation coil is [6]:

$$M_{ts} = M_0 \sum_{n=1}^{\infty} \sum_{m=2k+1}^{\infty} \alpha_{nm} \sin(mq_x X) e^{-\sqrt{a}Z} \sin[nq_y (Y+b)] \quad (1)$$

where, with finite thicknesses:

$$M_0 = \frac{128 \mu_0 N_s N_t}{\pi^2 s_s t_s s_t t_t q_y^5} \quad b = \frac{l_s + a}{2} y + t_s \quad (2)$$

$$\alpha_{nm} = \frac{1}{mn\sqrt{q}(q+n^2)}$$

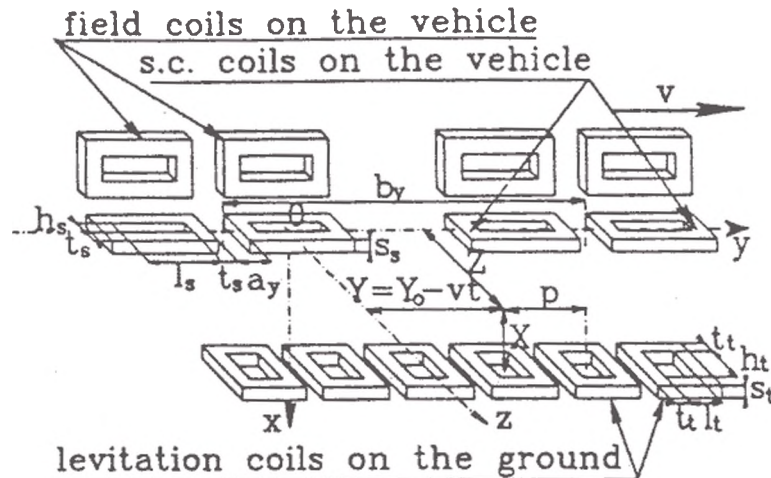


Fig. 3 - SC on-board and on-ground levitation coils on parallel and horizontal planes [Symbols as in Fig. 2].

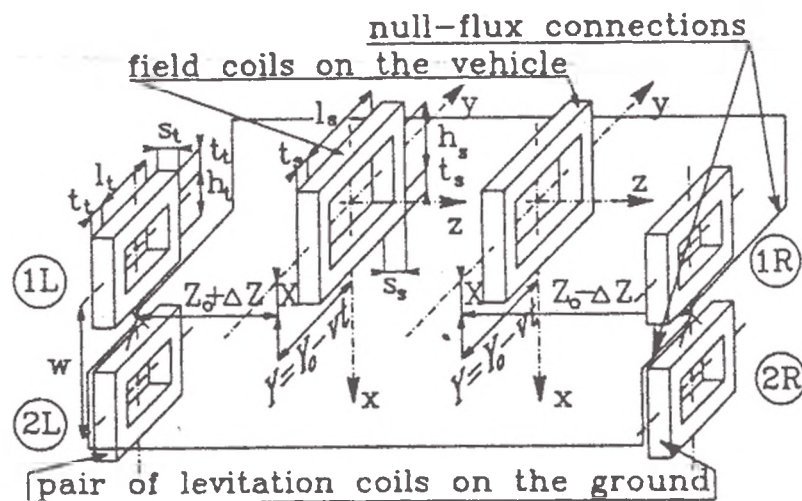


Fig. 4 - Field coils and pair of 8-shaped levitation coils on parallel and vertical planes [1L, 2L: left upper and lower unit coil; 1R, 2R: right upper and lower unit coil; X : coordinate of the center of an 8-shaped coil; W : distance between the centers of upper and lower unit coil; $Z_0 + \Delta Z$, $Z_0 - \Delta Z$: distance between 8-shaped coil and field coil, for the left and right side, respectively. Other symbols as in Fig. 2].

$$\begin{aligned} & \cdot \sinh\left(\sqrt{q} q_y \frac{s_s}{2}\right) \sin\left(m\delta q_y \frac{s_t}{2}\right) \sin(nq_y b) \cdot \\ & \cdot \left\{ \frac{1}{n-m\delta} \cos\left(nq_y \frac{l_s+t_s}{2} - m\delta q_y \frac{h_s+t_s}{2}\right) \sin\left[(n-m\delta)q_y \frac{t_s}{2}\right] - \right. \\ & \left. - \frac{1}{n+m\delta} \cos\left(nq_y \frac{l_s+t_s}{2} + m\delta q_y \frac{h_s+t_s}{2}\right) \sin\left[(n+m\delta)q_y \frac{t_s}{2}\right] \right\} \cdot \\ & \cdot \left\{ \frac{1}{n} \left[\cosh\left[\sqrt{q} q_y \left(\frac{h_t}{2} + t_t\right)\right] \sin\left[nq_y \left(\frac{l_t}{2} + t_t\right)\right] - \right. \right. \\ & \left. \left. - \cosh\left[\sqrt{q} q_y \frac{h_t}{2}\right] \sin\left(nq_y \frac{l_t}{2}\right) \right\} - \right. \\ & \left. - \frac{1}{\sqrt{q}} \left\{ \sinh\left[\sqrt{q} q_y \left(\frac{h_t}{2} + t_t\right)\right] \cos\left[nq_y \left(\frac{l_t}{2} + t_t\right)\right] - \right. \right. \\ & \left. \left. - \sinh\left[\sqrt{q} q_y \frac{h_t}{2}\right] \cos\left(nq_y \frac{l_t}{2}\right) \right\} \right\} , \end{aligned}$$

and, in the case of filiform coils:

$$M_0 = \frac{32 \mu_0 N_s N_t}{\pi^2 q_y} \quad b = \frac{l_s + a}{2} y \quad (3)$$

$$\alpha_{nm} = \frac{\delta}{n^2 \sqrt{q}} \sin(nq_y b) \sin\left(nq_y \frac{l_s}{2}\right) \sin\left(m\delta q_y \frac{h_s}{2}\right) \cdot \sin\left(nq_y \frac{l_t}{2}\right) \sinh\left(\sqrt{q} q_y \frac{h_t}{2}\right)$$

and where:

m, n generic harmonic along x and y , respectively
 N_s, N_t number of turns of field and levitation coils
 $q_x = \pi/g_x$ with g_x pitch of the series of fictitious field coils along x [5,6]

$$q_y = 2\pi/b_y \quad \delta = q_x/q_y$$

$$q = n^2 + m^2 \delta^2 \quad a = q q_y^2$$

The induced current in the generic levitation coil is [7]:

$$i_t(t) = \frac{M_o I_s}{L} \sum_{n=1}^{\infty} \sum_{k=0}^{\infty} \frac{n \alpha_{nm} \lambda_n Q}{\sqrt{1+(n\lambda_n Q)^2}} \sin(mq_x X) \cdot e^{-\sqrt{a}Z} \cos\left[nq_y(Y+b) + \arctg(n\lambda_n Q)\right] \quad (4)$$

being:

$$Q = \frac{q_y v L}{R} \quad \lambda_n = \frac{\Omega_n}{L}$$

where I_s is the field current, R and L the resistance and the self inductance of a levitation coil and Ω_n a fictitious self inductance taking into account, unlike [5], the mutual linkage with the other levitation coils of the series [7].

The components F_{xt} , F_{yt} , F_{zt} of the force acting on a levitation coil, equal and opposed to the levitation, drag and lateral forces that the coil causes on the vehicle, are in general:

$$F_{xt} = \frac{\partial M_{ts}}{\partial X} I_s i_t(t) \quad (5)$$

$$F_{yt} = \frac{\partial M_{ts}}{\partial Y} I_s i_t(t) \quad (6)$$

$$F_{zt} = \frac{\partial M_{ts}}{\partial Z} I_s i_t(t) \quad (7)$$

Levitation force

From (5), with the positions:

$$\bar{R}_n = - \sum_{k=0}^{\infty} \sum_{m=2k+1}^{\infty} 2\pi m \delta \alpha_{nm} \cos(mq_x X) e^{-\sqrt{a}Z} \quad (8)$$

$$S_n = \sum_{k=0}^{\infty} \sum_{m=2k+1}^{\infty} \alpha_{nm} \sin(mq_x X) e^{-\sqrt{a}Z} \quad (9)$$

the instantaneous value is obtained [7]:

$$F_{xt} = - \frac{(M_o I_s)^2}{2b_y L} \sum_{n=1}^{\infty} \sum_{n'=1}^{\infty} \frac{n' R S_n \lambda_n Q}{\sqrt{1+(n'\lambda_n Q)^2}} \cdot \left\{ \sin\left[(n+n')q_y(Y+b) + \arctg(n'\lambda_n Q)\right] + \sin\left[(n-n')q_y(Y+b) - \arctg(n'\lambda_n Q)\right] \right\} \quad (10)$$

Putting $n=n'$ in (10), the mean value in time is obtained:

$$\langle F_{xt} \rangle = \frac{(M_o I_s)^2}{2b_y L} \sum_{n=1}^{\infty} R S_n \frac{(n\lambda_n Q)^2}{1+(n\lambda_n Q)^2} \quad (11)$$

The levitation force F_x caused by the levitation coil on the vehicle is given, due to the principle of action and reaction, by (10) and (11) with the sign changed.

For Q sufficiently high, it results that:

$$\frac{(n\lambda_n Q)^2}{1+(n\lambda_n Q)^2} \approx 1$$

It follows that, at high speed and with other conditions unchanged, the mean levitation force is nearly independent of the speed itself.

Drag force

In a similar way, from (6) the instantaneous value is obtained [7]:

$$F_{yt} = \frac{(M_o I_s)^2}{2b_y L} \sum_{n=1}^{\infty} \sum_{n'=1}^{\infty} \frac{2\pi n' S_n \lambda_n Q}{\sqrt{1+(n'\lambda_n Q)^2}} \cdot \left\{ \cos\left[(n+n')q_y(Y+b) + \arctg(n'\lambda_n Q)\right] + \cos\left[(n-n')q_y(Y+b) - \arctg(n'\lambda_n Q)\right] \right\} \quad (12)$$

Putting $n=n'$ in (12), the mean value is obtained:

$$\langle F_{yt} \rangle = \frac{(M_o I_s)^2}{2b_y L} \sum_{n=1}^{\infty} S_n^2 \frac{2\pi n^2 \lambda_n Q}{1+(n\lambda_n Q)^2} \quad (13)$$

Viewing the terms of the sum in (13), it comes out that the sign of $\langle F_{yt} \rangle$ is the sign of Q and therefore of v ; it follows that, due to the principle of action and reaction, the sign of the force $\langle F_y \rangle$ caused by the levitation coil on the vehicle is opposed and therefore such a force is a drag force. Furthermore, for Q sufficiently high, $\langle F_{yt} \rangle$ decreases nearly with $1/Q$ and therefore with $1/v$.

The absolute value of the ratio between $\langle F_x \rangle$ and $\langle F_y \rangle$ (drag ratio) estimates the efficiency of the levitation system: the higher it is, the lower the drag force, the levitation force being equal. From (11) and (13) it results that:

$$dr = \left| \frac{\langle F_x \rangle}{\langle F_y \rangle} \right| = \left| \frac{\sum_1^\infty R_n S_n \frac{(n\lambda_n)^2}{Q^2 + (n\lambda_n)^2}}{\sum_1^\infty S_n^2 \frac{2\pi m^2 \lambda_n}{Q^2 + (n\lambda_n)^2}} \right| |Q| \quad (14)$$

For Q sufficiently high, dr is nearly proportional to $|Q|$ and therefore to $|v|$, the geometrical and electrical characteristics of the coils being unchanged.

Lateral force

From (7), with the position:

$$T_n = \sum_{\substack{m=2k+1 \\ k=0}}^\infty 2\pi\sqrt{q} \alpha_{nm} \sin(mq_x X) e^{-\sqrt{a}Z} \quad (15)$$

the instantaneous value is obtained:

$$F_{zt} = -\frac{(M_o I_s)^2}{2b_y L} \sum_1^\infty \sum_{n'}^\infty \frac{n' T_n S_{n'} \lambda_n Q}{\sqrt{1+(n'\lambda_n Q)^2}} \cdot \left\{ \sin\left[\left(n+n'\right)q_y(Y+b) + \arctg(n'\lambda_n Q)\right] + \sin\left[\left(n-n'\right)q_y(Y+b) - \arctg(n'\lambda_n Q)\right] \right\} \quad (16)$$

Putting $n=n'$ in (16), the mean value is obtained:

$$\langle F_{zt} \rangle = \frac{(M_o I_s)^2}{2b_y L} \sum_1^\infty T_n S_n \frac{(n\lambda_n Q)^2}{1+(n\lambda_n Q)^2} \quad (17)$$

The lateral force F_z acting on the vehicle is given, due to the principle of action and reaction, by (16) and (17) with the sign changed.

From (10), (12) and (16) the time harmonics of the forces F_x , F_y and F_z can be obtained [7].

4 Forces between coils on parallel and horizontal planes

With reference to Fig.3, the coefficient M_{ts} is given by [6]:

$$M_{ts} = M_o \sum_1^\infty \sum_{\substack{m=2k+1 \\ k=0}}^\infty \alpha_{nm} \cos(mq_z Z) e^{-\sqrt{a}X} \sin[nq_y(Y+b)] \quad (18)$$

where, with finite thicknesses (M_o and b are given by (2)):

$$\alpha_{nm} = \frac{1}{\delta m^2 n^2 \sqrt{q}} \cdot \sinh\left(\sqrt{q}q_y \frac{s}{2}\right) \sinh\left(\sqrt{q}q_y \frac{t}{2}\right) \sin(nq_y b) \cdot \left\{ \frac{1}{n-m\delta} \cos\left(nq_y \frac{l_s+t_s}{2} - m\delta q_y \frac{h_s+t_s}{2}\right) \sin\left[\left(n-m\delta\right)q_y \frac{t_s}{2}\right] - \frac{1}{n+m\delta} \cos\left(nq_y \frac{l_s+t_s}{2} + m\delta q_y \frac{h_s+t_s}{2}\right) \sin\left[\left(n+m\delta\right)q_y \frac{t_s}{2}\right] \right\}$$

$$\cdot \left\{ \frac{1}{n-m\delta} \cos\left(nq_y \frac{l_t+t_t}{2} - m\delta q_y \frac{h_t+t_t}{2}\right) \sin\left[\left(n-m\delta\right)q_y \frac{t_t}{2}\right] - \frac{1}{n+m\delta} \cos\left(nq_y \frac{l_t+t_t}{2} + m\delta q_y \frac{h_t+t_t}{2}\right) \sin\left[\left(n+m\delta\right)q_y \frac{t_t}{2}\right] \right\}$$

and, in the case of filiform coils (M_o and b are given by (3)):

$$\alpha_{nm} = \frac{\sqrt{q}}{\delta m^2 n^2} \sin(nq_y b) \sin\left(nq_y \frac{l_s}{2}\right) \sin\left(m\delta q_y \frac{h_s}{2}\right) \cdot \sin\left(nq_y \frac{l_t}{2}\right) \sin\left(m\delta q_y \frac{h_t}{2}\right)$$

and where:

$$q_z = \pi/g_z \quad \text{with } g_z \text{ pitch of the series of fictitious field coils along } z \text{ [5,6]}$$

$$\delta = q_z/q_y$$

The induced current in the generic levitation coil is now given by [7]:

$$i_t(t) = \frac{M_o I_s}{L} \sum_1^\infty \sum_{\substack{m=2k+1 \\ k=0}}^\infty \frac{n \alpha_{nm} \lambda_n Q}{\sqrt{1+(n\lambda_n Q)^2}} \cos(mq_z Z) \cdot e^{-\sqrt{a}X} \cos\left[nq_y(Y+b) + \arctg(n\lambda_n Q)\right] \quad (19)$$

With the positions:

$$R_n = \sum_{\substack{m=2k+1 \\ k=0}}^\infty 2\pi\sqrt{q} \alpha_{nm} \cos(mq_z Z) e^{-\sqrt{a}X}$$

$$S_n = \sum_{\substack{m=2k+1 \\ k=0}}^\infty \alpha_{nm} \cos(mq_z Z) e^{-\sqrt{a}X}$$

$$T_n = \sum_{\substack{m=2k+1 \\ k=0}}^\infty 2\pi m \delta \alpha_{nm} \sin(mq_z Z) e^{-\sqrt{a}X}$$

equations (10)+(14) may be applied also in this case.

5 Forces between coils on parallel and vertical planes

With reference to Fig.4, the null-flux connection between the 8-shaped coils on both sides of the guideway may be represented by the circuit of Fig.5a, where [6]:

$$\begin{aligned} e_{1L} &= e_L + \Delta e_L = -\frac{\partial M_{1L}}{\partial Y} I_o v \\ e_{2L} &= e_L - \Delta e_L = -\frac{\partial M_{2L}}{\partial Y} I_o v \\ e_{1R} &= e_R + \Delta e_R = -\frac{\partial M_{1R}}{\partial Y} I_o v \\ e_{2R} &= e_R - \Delta e_R = -\frac{\partial M_{2R}}{\partial Y} I_o v \end{aligned} \quad (20)$$

$$\begin{aligned} i_{1L} &= i_L + \Delta i_L & i_{2L} &= i_L - \Delta i_L \\ i_{1R} &= i_R + \Delta i_R & i_{2R} &= i_R - \Delta i_R \end{aligned}$$

from which:

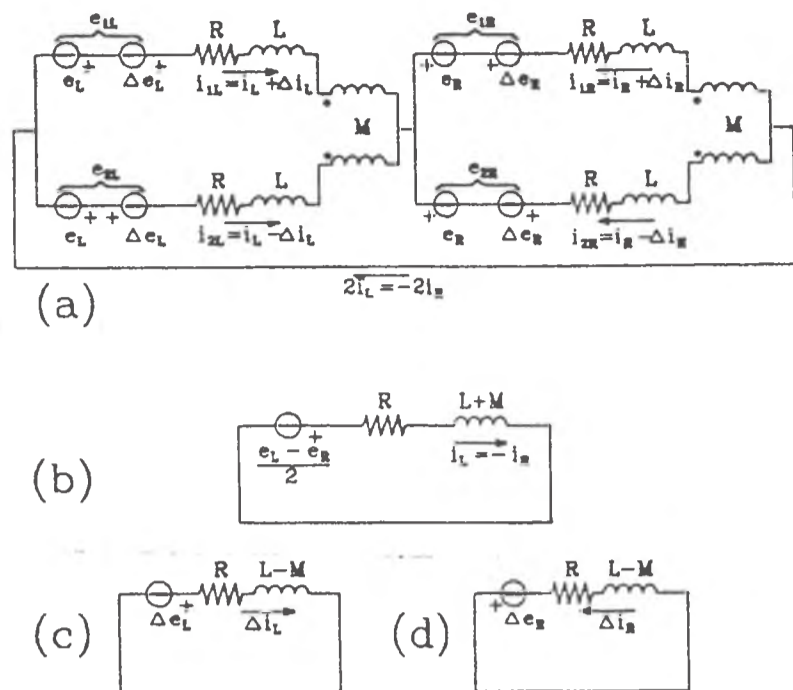


Fig.5 - Equivalent circuit of the levitation coil system of Fig.4 (a) and resolution into the circuits (b), (c) and (d) [e_{ij} , i_{ij} : e.m.f.s and currents of unit coil ij ; R , L : resistance and self inductance of a unit coil; M : mutual inductance between upper and lower unit coil].

$$\begin{aligned}
 e_L &= \frac{e_{1L} + e_{2L}}{2} = -\frac{\partial}{\partial Y} \left(\frac{M_{1L} + M_{2L}}{2} \right) I_s v \\
 \Delta e_L &= \frac{e_{1L} - e_{2L}}{2} = -\frac{\partial}{\partial Y} \left(\frac{M_{1L} - M_{2L}}{2} \right) I_s v \\
 e_R &= \frac{e_{1R} + e_{2R}}{2} = -\frac{\partial}{\partial Y} \left(\frac{M_{1R} + M_{2R}}{2} \right) I_s v \\
 \Delta e_R &= \frac{e_{1R} - e_{2R}}{2} = -\frac{\partial}{\partial Y} \left(\frac{M_{1R} - M_{2R}}{2} \right) I_s v \\
 i_L &= \frac{i_{1L} + i_{2L}}{2} & i_R &= \frac{i_{1R} + i_{2R}}{2} \\
 \Delta i_L &= \frac{i_{1L} - i_{2L}}{2} & \Delta i_R &= \frac{i_{1R} - i_{2R}}{2}
 \end{aligned} \tag{21}$$

With the positions:

$$\begin{aligned}
 M_L &= \frac{M_{1L} - M_{2L}}{2} & M_R &= \frac{M_{1R} - M_{2R}}{2} \\
 M_G &= \frac{M_{1L} + M_{2L} - M_{1R} - M_{2R}}{4}
 \end{aligned} \tag{22}$$

and applying the principle of superposition of effects, the analysis of such a circuit may be separated in that of the circuit of Fig.5b, where:

$$\frac{e_L - e_R}{2} = -\frac{\partial M_G}{\partial Y} I_s v$$

and in that of the circuits of Fig.5c e 5d, where:

$$\Delta e_L = -\frac{\partial M_L}{\partial Y} I_s v \quad \Delta e_R = -\frac{\partial M_R}{\partial Y} I_s v$$

It is [6]:

$$\begin{aligned}
 M_L &= M_0 \sum_{n=1}^{\infty} \sum_{m=2k+1}^{\infty} \mathcal{X}_{nm} \sin\left(mq_x \frac{W}{2}\right) \cdot \\
 &\quad \sin\left(mq_x X\right) e^{-\sqrt{a}(Z_0 + \Delta Z)} \sin[nq_y(Y+b)] \\
 M_R &= M_0 \sum_{n=1}^{\infty} \sum_{m=2k+1}^{\infty} \mathcal{X}_{nm} \sin\left(mq_x \frac{W}{2}\right) \cdot \\
 &\quad \sin\left(mq_x X\right) e^{-\sqrt{a}(Z_0 - \Delta Z)} \sin[nq_y(Y+b)] \\
 M_G &= -M_0 \sum_{n=1}^{\infty} \sum_{m=2k+1}^{\infty} \mathcal{X}_{nm} \cos\left(mq_x \frac{W}{2}\right) \cdot \\
 &\quad \cos\left(mq_x X\right) e^{-\sqrt{a}Z_0} \sinh(\sqrt{a}\Delta Z) \sin[nq_y(Y+b)]
 \end{aligned}$$

where the expressions for M_0 , b and \mathcal{X}_{nm} are those given in §4, provided q_x replaces now q_z .

With reference to the circuit of Fig.5b, the induced current $i_L = -i_R$ is given by [7]:

$$\begin{aligned}
 i_L &= -\frac{M_0 I_s}{L+M} \sum_{n=1}^{\infty} \sum_{m=2k+1}^{\infty} \frac{n \mathcal{X}_{nm} \lambda'_n Q'}{\sqrt{1 + (n\lambda'_n Q')^2}} \cdot \\
 &\quad \cos\left(mq_x \frac{W}{2}\right) \cos\left(mq_x X\right) e^{-\sqrt{a}Z_0} \sinh(\sqrt{a}\Delta Z) \cdot \\
 &\quad \cos\left[nq_y(Y+b) + \arctg(n\lambda'_n Q')\right]
 \end{aligned} \tag{23}$$

with the positions:

$$\lambda'_n = \frac{\Omega'_n}{L+M} \quad Q = \frac{q_y v (L+M)}{R}$$

Ω'_n is a fictitious self inductance which takes into account, besides the mutual linking with the unit coils of the same row, also the mutual linking between the upper unit coils and the lower ones, bearing in mind the sign conventions of Fig.5a [7].

In a similar way, the currents flowing in the circuits of Fig.5c and 5d are given by [7]:

$$\begin{aligned}
 \Delta i_L &= \frac{M_0 I_s}{L-M} \sum_{n=1}^{\infty} \sum_{m=2k+1}^{\infty} \frac{n \mathcal{X}_{nm} \lambda''_n Q''}{\sqrt{1 + (n\lambda''_n Q'')^2}} \cdot \\
 &\quad \sin\left(mq_x \frac{W}{2}\right) \sin\left(mq_x X\right) e^{-\sqrt{a}(Z_0 + \Delta Z)} \cdot \\
 &\quad \cos\left[nq_y(Y+b) + \arctg(n\lambda''_n Q'')\right]
 \end{aligned} \tag{24}$$

$$\begin{aligned}
 \Delta i_R &= \frac{M_0 I_s}{L-M} \sum_{n=1}^{\infty} \sum_{m=2k+1}^{\infty} \frac{n \mathcal{X}_{nm} \lambda''_n Q''}{\sqrt{1 + (n\lambda''_n Q'')^2}} \cdot \\
 &\quad \sin\left(mq_x \frac{W}{2}\right) \sin\left(mq_x X\right) e^{-\sqrt{a}(Z_0 - \Delta Z)} \cdot \\
 &\quad \cos\left[nq_y(Y+b) + \arctg(n\lambda''_n Q'')\right]
 \end{aligned} \tag{25}$$

with the positions:

$$\lambda_n'' = \frac{\Omega_n''}{L-M} \quad Q'' = \frac{q_y v(L-M)}{R}$$

bearing in mind that $\Omega_n'' \neq \Omega_n'$, because the contribution of the mutual linkage between upper and lower unit coils has in this case opposed sign with respect to the circuit of Fig.5b.

The component along x of the force acting on a pair of 8-shaped coils (Fig.4) is:

$$F_{xt} = \frac{\partial M_{1L}}{\partial X} I_s i_{1L} + \frac{\partial M_{2L}}{\partial X} I_s i_{2L} + \frac{\partial M_{1R}}{\partial X} I_s i_{1R} + \frac{\partial M_{2R}}{\partial X} I_s i_{2R}$$

that is:

$$F_{xt} = 4 \frac{\partial M_G}{\partial X} I_s i_L + 2 \frac{\partial M_L}{\partial X} I_s \Delta i_L + 2 \frac{\partial M_R}{\partial X} I_s \Delta i_R \quad (26)$$

Similarly, the other two components are:

$$F_{yt} = 4 \frac{\partial M_G}{\partial Y} I_s i_L + 2 \frac{\partial M_L}{\partial Y} I_s \Delta i_L + 2 \frac{\partial M_R}{\partial Y} I_s \Delta i_R \quad (27)$$

$$F_{zt} = 4 \frac{\partial M_G}{\partial \Delta Z} I_s i_L + 2 \frac{\partial M_L}{\partial \Delta Z} I_s \Delta i_L + 2 \frac{\partial M_R}{\partial \Delta Z} I_s \Delta i_R \quad (28)$$

Equations (26)+(28) may be expressed in vectorial form:

$$\bar{F}_t = \bar{F}_{Gt} + \bar{F}_{Lt} + \bar{F}_{Rt}$$

where \bar{F}_{Gt} , \bar{F}_{Lt} and \bar{F}_{Rt} are the contributions, due to the circuits of Fig.5b, 5c and 5d, to the total force \bar{F}_t acting on the pair of 8-shaped coils. It is:

$$\begin{aligned} \bar{F}_{Gt} &= \left\{ F_{Gxt}, F_{Gyt}, F_{Gzt} \right\} \\ &= \left\{ 4 \frac{\partial M_G}{\partial X} I_s i_L, 4 \frac{\partial M_G}{\partial Y} I_s i_L, 4 \frac{\partial M_G}{\partial \Delta Z} I_s i_L \right\} \end{aligned}$$

and similarly:

$$\begin{aligned} \bar{F}_{Lt} &= \left\{ 2 \frac{\partial M_L}{\partial X} I_s \Delta i_L, 2 \frac{\partial M_L}{\partial Y} I_s \Delta i_L, 2 \frac{\partial M_L}{\partial \Delta Z} I_s \Delta i_L \right\} \\ \bar{F}_{Rt} &= \left\{ 2 \frac{\partial M_R}{\partial X} I_s \Delta i_R, 2 \frac{\partial M_R}{\partial Y} I_s \Delta i_R, 2 \frac{\partial M_R}{\partial \Delta Z} I_s \Delta i_R \right\} \end{aligned}$$

In the case of Fig.5b a dynamic effect is present only if $i_L \neq 0$, that is only if $\Delta Z \neq 0$: the current flowing in the null-flux connection produces the force \bar{F}_{Gt} . The circuits of Fig.5c and 5d take into account the left and right 8-shaped coil respectively, on which the forces \bar{F}_{Lt} and \bar{F}_{Rt} act.

Expressions (10)+(14) may be again applied to the components of \bar{F}_{Gt} , \bar{F}_{Lt} and \bar{F}_{Rt} , provided a different formulation for R_n , S_n and T_n is given. With the positions:

$$R_{Ln} = - \sum_{k=0}^{\infty} 2\pi m \delta \mathcal{X}_{nm} \sin\left(mq \frac{W}{2}\right) \cos(mq_x X) e^{-\sqrt{a}(Z_0 + \Delta Z)}$$

$$\begin{aligned} S_{Ln} &= \sum_{k=0}^{\infty} \mathcal{X}_{nm} \sin\left(mq \frac{W}{2}\right) \sin(mq_x X) e^{-\sqrt{a}(Z_0 + \Delta Z)} \\ T_{Ln} &= \sum_{k=0}^{\infty} 2\pi\sqrt{q} \mathcal{X}_{nm} \sin\left(mq \frac{W}{2}\right) \sin(mq_x X) e^{-\sqrt{a}(Z_0 + \Delta Z)} \\ R_{Rn} &= - \sum_{k=0}^{\infty} 2\pi m \delta \mathcal{X}_{nm} \sin\left(mq \frac{W}{2}\right) \cos(mq_x X) e^{-\sqrt{a}(Z_0 - \Delta Z)} \\ S_{Rn} &= \sum_{k=0}^{\infty} \mathcal{X}_{nm} \sin\left(mq \frac{W}{2}\right) \sin(mq_x X) e^{-\sqrt{a}(Z_0 - \Delta Z)} \\ T_{Rn} &= - \sum_{k=0}^{\infty} 2\pi\sqrt{q} \mathcal{X}_{nm} \sin\left(mq \frac{W}{2}\right) \sin(mq_x X) e^{-\sqrt{a}(Z_0 - \Delta Z)} \\ R_{Gn} &= - \sum_{k=0}^{\infty} 2\pi m \delta \mathcal{X}_{nm} \cos\left(mq \frac{W}{2}\right) \cdot \\ &\quad \cdot \sin(mq_x X) e^{-\sqrt{a}Z_0} \sinh(\sqrt{a}\Delta Z) \\ S_{Gn} &= - \sum_{k=0}^{\infty} \mathcal{X}_{nm} \cos\left(mq \frac{W}{2}\right) \cos(mq_x X) e^{-\sqrt{a}Z_0} \sinh(\sqrt{a}\Delta Z) \\ T_{Gn} &= \sum_{k=0}^{\infty} 2\pi\sqrt{q} \mathcal{X}_{nm} \cos\left(mq \frac{W}{2}\right) \cdot \\ &\quad \cdot \cos(mq_x X) e^{-\sqrt{a}Z_0} \cosh(\sqrt{a}\Delta Z) \end{aligned}$$

the time harmonics of \bar{F}_{Gt} , \bar{F}_{Lt} and \bar{F}_{Rt} can be therefore obtained.

The time mean values of the components are [7]:

$$\langle F_{ixt} \rangle = \frac{(M_o I_s)^2}{2b_y L_i} \sum_1^n R_{in} S_{in} \frac{(n\lambda_{in} Q_i)^2}{1 + (n\lambda_{in} Q_i)^2} \quad (29)$$

$$\langle F_{iyt} \rangle = \frac{(M_o I_s)^2}{2b_y L_i} \sum_1^n S_{in}^2 \frac{2\pi m^2 \lambda_{in} Q_i}{1 + (n\lambda_{in} Q_i)^2} \quad (30)$$

$$\langle F_{izt} \rangle = \frac{(M_o I_s)^2}{2b_y L_i} \sum_1^n T_{in} S_{in} \frac{(n\lambda_{in} Q_i)^2}{1 + (n\lambda_{in} Q_i)^2} \quad (31)$$

where $i=G, L, R$, $L_G=L+M$, $L_R=L-L-M$, $\lambda_{Gn}=\lambda_n'$, $\lambda_{Rn}=\lambda_{Ln}=\lambda_n''$, $Q_G=Q'$ e $Q_R=Q_L=Q''$. Again, for Q' and Q'' sufficiently high, the drag ratio dr is nearly proportional to the speed.

Finally, the total mean forces are:

$$\begin{aligned} \langle F_{xt} \rangle &= \langle F_{Gxt} \rangle + \langle F_{Lxt} \rangle + \langle F_{Rxt} \rangle \\ \langle F_{yt} \rangle &= \langle F_{Gyt} \rangle + \langle F_{Lyt} \rangle + \langle F_{Ryt} \rangle \\ \langle F_{zt} \rangle &= \langle F_{Gzt} \rangle + \langle F_{Lzt} \rangle + \langle F_{Rzt} \rangle \end{aligned} \quad (32)$$

while the levitation $\langle F_x \rangle$, drag $\langle F_y \rangle$ and lateral $\langle F_z \rangle$ forces acting on the vehicle and produced by the pair of 8-shaped coils are given by (32) with the sign changed.

Important quantities for the stability analysis are the incremental forces $\partial \langle F_{xt} \rangle / \partial X$ and $\partial \langle F_{zt} \rangle / \partial \Delta Z$, obtained by the derivation of R_{in} ,

S_{in}, T_{in} : The vertical and lateral stabilities of the vehicle are possible if:

$$\left. \frac{\partial \langle F_{xt} \rangle}{\partial X} \right|_{X=X_0} < 0 \quad \left. \frac{\partial \langle F_{zt} \rangle}{\partial \Delta Z} \right|_{\Delta Z=0} > 0$$

being X_0 the coordinate of the equilibrium point between the levitation force and the weight of the vehicle.

In all the configurations, the mean forces per polar pair acting on the vehicle are 2N times the forces produced by a single coil or N times the forces produced by a pair of 8-shaped coils. As for the harmonics, in the forces per polar pair are present only harmonics with angular frequency $Nq\omega$ and multiple and amplitude 2N (N) times that of a single coil (pair of 8-shaped coils) [7].

6 Examples of application

Field and levitation coils on orthogonal planes

The expressions developed in §3 have been utilized to calculate the levitation, drag and lateral forces acting on an EDS-MAGLEV vehicle with the coil configuration of Fig.2. With reference to the data of Tab.I, Fig.6 gives the instantaneous forces acting on a levitation coil for $Z=Z_0$ and $v=500$ km/h.

Tab.I - Geometrical and electrical parameters of a vehicle with the configuration of Fig.2

$l_g = 1.9$ m	$h = 0.45$ m	$t = 0.05$ m
$s_g = 0.08$ m	$N_g = 1200$	$I_g = 600$ A
$a = 0.7$ m	$b = 21.6$ m	
$l_t = 0.53$ m	$h_t = 0.23$ m	$t_t = 0.07$ m
$s_t = 0.09$ m	$N_t = 52$	$Z_0 = 0.25$ m
$N = 24$	$R = 35$ mΩ	$L = 1.73$ mH

Vehicle weight = 178 kN
Polar pairs per vehicle and side = 1

Fig.7 gives the mean forces acting on a coil versus X. As a single coil has to produce a mean levitation force of 3.7 kN in order to balance the vehicle weight, from Fig.7 one can deduce that at 500 km/h the balance displacement is $X_0=0.411$ m. Furthermore, near such a point it results that $(\partial \langle F_{xt} \rangle / \partial X) < 0$ and therefore the vehicle is inherently stable in the vertical direction; on the contrary it is possible to verify that it results that $(\partial \langle F_{zt} \rangle / \partial \Delta Z) > 0$ and therefore the vehicle is inherently unstable in the lateral direction and a control is necessary to get stability. Finally, Fig.8 gives the mean forces $\langle F_{yt} \rangle$ and $\langle F_{zt} \rangle$ acting on a coil, the drag ratio, the r.m.s. induced current and the balance displacement X_0 versus speed.

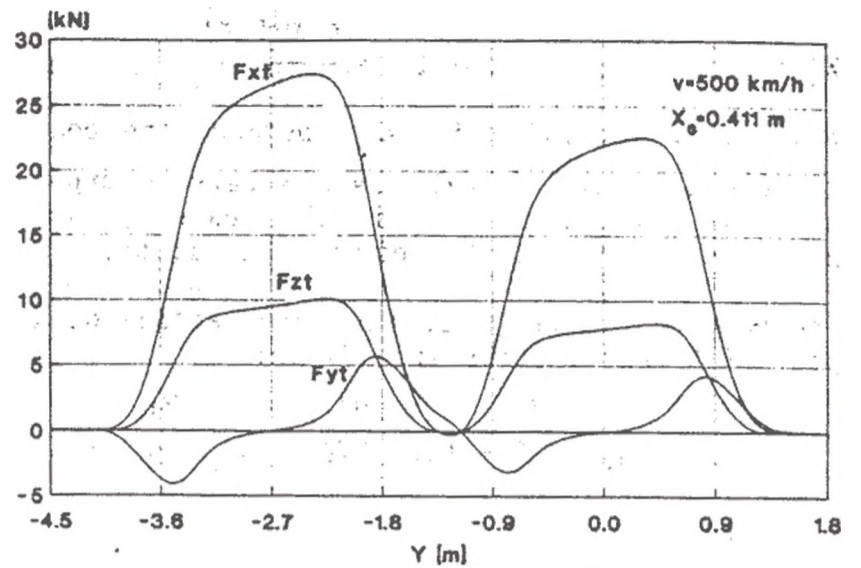


Fig.6 - Instantaneous values of levitation F_{xt} , drag F_{yt} and lateral F_{zt} forces acting on a levitation coil versus Y (Configuration of Fig.2 and Tab.I) [$m=51$; $n=71$; $g_x=3.5$ m].

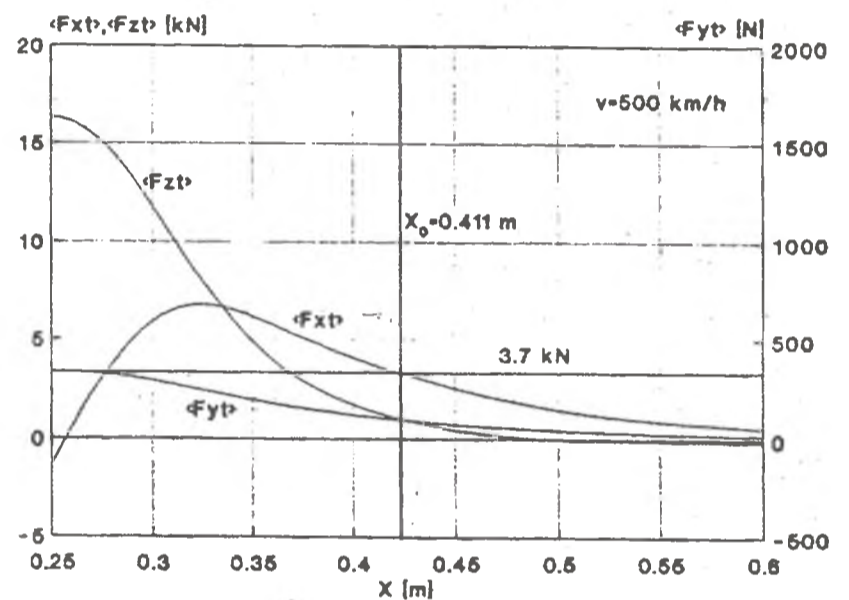


Fig.7 - Mean levitation $\langle F_{xt} \rangle$, drag $\langle F_{yt} \rangle$ and lateral $\langle F_{zt} \rangle$ forces acting on a levitation coil versus X (Configuration of Fig.2 and Tab.I).

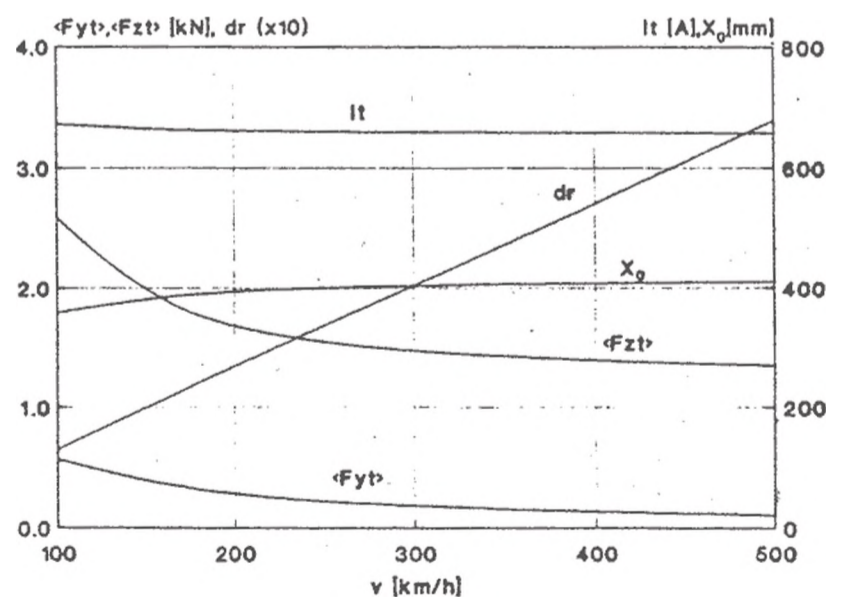


Fig.8 - Mean drag $\langle F_{yt} \rangle$ and lateral $\langle F_{zt} \rangle$ forces acting on a levitation coil, drag ratio, induced current and balance displacement versus speed (Configuration of Fig.2 and Tab.I).

Field and levitation coils on parallel and vertical planes

The expressions developed in §5 have been utilized to calculate the levitation, drag and lateral forces acting on an EDS-MAGLEV vehicle with the coil configuration of Fig.4. With reference to the data of Tab.II [4,8], Fig.9 gives the instantaneous forces acting on a pair of 8-shaped coils for $\Delta Z=0$ at $v=500$ km/h.

Tab.II - Geometrical and electrical parameters of a vehicle with the configuration of Fig.4

$l_s = 2.15$ m	$h_s = 0.45$ m	$t_s = 0.05$ m
$s_s = 0.08$ m	$N_s = 1000$	$I_s = 700$ A
$a_y = 0.45$	$b_y = 21.6$ m	
$l_t = 0.73$ m	$h_t = 0.27$ m	$t_t = 0.07$ m
$s_t = 0.09$ m	$N_t = 52$	
$W = 0.42$ m	$Z_o = 0.185$ m	$N = 24$
$R = 45$ m Ω	$L = 2.33$ mH	$M = -0.31$ mH

Vehicle weight = 200 kN
Polar pairs per vehicle and side = 1

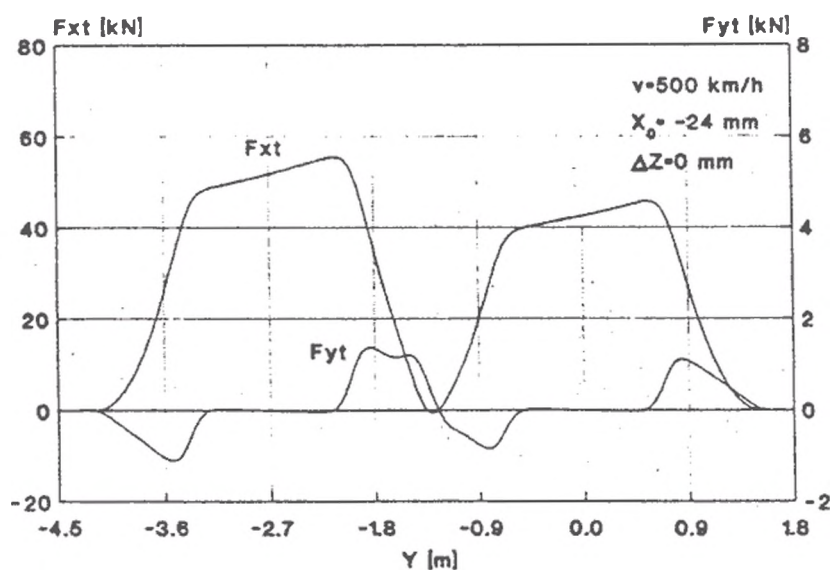


Fig.9 - Instantaneous levitation F_{xt} and drag F_{yt} forces acting on a pair of 8-shaped coil versus Y (Configuration of Fig.4 and Tab.II) [$m=201$; $n=201$; $g_x=3.5$ m].

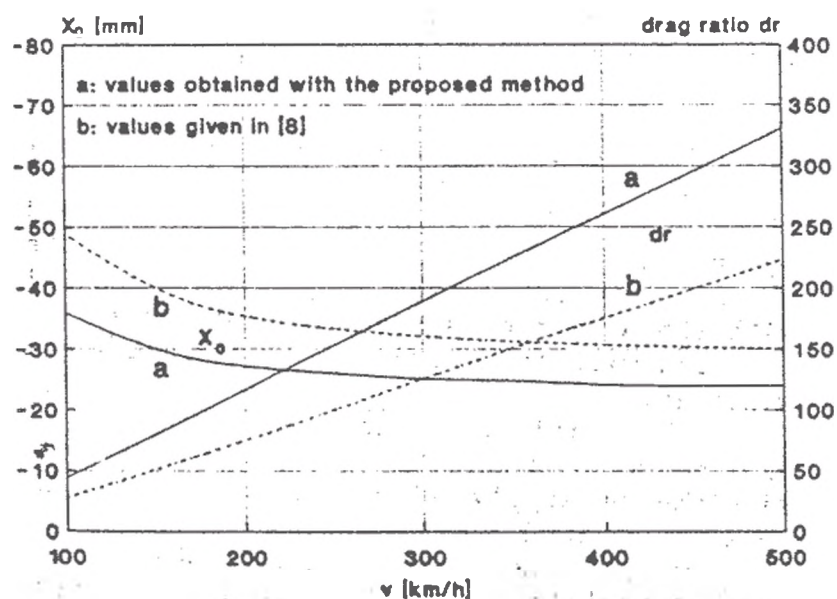


Fig.10 - Balance displacement and drag ratio versus speed (Configuration of Fig.4 e Tab.II).

Finally, Fig.10 gives the balance displacement X_o and the drag ratio dr versus speed and compares the obtained results with the ones in [8].

The above diagrams have been obtained with the approximation of filiform coils; the calculations, repeated taking into account the coil finite thicknesses, have given results some percent different from the previous ones.

7 Conclusion

The levitation, drag and lateral forces, obtained in the paper using an analytical three-dimensional method, are formulated by means of general expressions; this allows their application to all the different coil configurations proposed for EDS-MAGLEV systems with SC magnets and air-core LSM.

The developed expressions can be applied both to the actual case of coils with finite thicknesses and to the approximated case of filiform coils, allowing simpler expressions with a usually satisfactory precision. The developed expressions also take into account the mutual linkage between levitation coils of a row. Finally, the utilization of analytically-developed general expressions allows to perform, unlike numerical methods, a quick and easy evaluation of the forces when the coil sizes and configurations vary.

References

- [1] G.Martinelli, A.Morini, *Potential Markets and Economic Considerations for High-Speed MAGLEV Transportation*, I° ETTIAS (European Training on Technologies and Industrial Applications of Superconductivity), Naples, Italy, Sept.1991.
- [2] G.Martinelli, A.Morini, *High-Speed Transportation and Superconducting Technology*, I° ETTIAS, Naples, Italy, Sept.1991.
- [3] Y.Kyotani, *Recent Progress by JNR on MAGLEV*, IEEE Trans. on Magn. MAG-24 (1988).
- [4] T.Doi, A.Seki, M.Uno, *The Linear Express*, 11th Int. Conf. on Magnetically Levitated Systems and Linear Drives, Yokohama, Japan, July 1989.
- [5] N.Carbonari, G.Martinelli, A.Morini, *Calculation of Levitation, Drag and Lateral Forces in EDS-MAGLEV Transport Systems*, Archiv für Elektrotechnik, 71 (1988).
- [6] F.Albicini, M.Andriollo, G.Martinelli, A.Morini, *EDS-MAGLEV Systems: Three-dimensional analytical method for the calculation of inductance coefficients*, Internal Report UPDie 92/02, March 1992.
- [7] M.Andriollo, G.Martinelli, A.Morini, A.Scuttari, *EDS-MAGLEV Systems: Three-dimensional analytical method for the calculation of forces*, Internal Report UPDie 92/03, March 1992.
- [8] S.Fujiwara, T.Fujimoto, *Characteristics of the combined levitation and guidance system using ground coils on the side wall of the guideway*, 11th Int. Conf. on Magnetically Levitated Systems and Linear Drives, Yokohama, Japan, July 1989.